Tracking the early dispersion of contaminated sediment along rivers draining the Fukushima radioactive pollution plume

Caroline Chartin, O. Evrard, Yuichi Onda, Jérémy Patin, Irène Lefevre, Catherine Ottle, Sophie Ayrault, Hugo Lepage, Philippe Bonté

Tracking the early dispersion of contaminated sediment along rivers draining the Fukushima radioactive pollution plume

Caroline Chartin[a], *Olivier Evrard*[a,*], *Yuichi Onda*[b,*], *Jeremy Patin*[b], *Irène Lefèvre*[a], *Catherine Ottlé*[a], *Sophie Ayrault*[a], *Hugo Lepage*[a], *Philippe Bonté*[a]

AUTHOR ADDRESSES

[a] Laboratoire des Sciences du Climat et de l'Environnement (LSCE/IPSL), Unité Mixte de Recherche 8212 (CEA, CNRS, UVSQ), 91198, Gif-sur-Yvette Cedex, France

[b] Center for Research in Isotopes and Environmental Dynamics (CRIED), University of Tsukuba, 1-1-1 Tennodai, Tsukuba, Ibaraki 305-8572, Japan

[*] Corresponding authors.

E-mail addresses: olivier.evrard@lsce.ipsl.fr (O. Evrard); onda@geoenv.tsukuba.ac.jp (Y. Onda)

Keywords: erosion; sediment; river catchments; contamination; transfer

ABSTRACT

Soil erosion and subsequent sediment transport in rivers play a major role in the global biogeochemical cycles and on the dispersion of contaminants within the natural environment. As other particle-borne pollutants, fallout radionuclides emitted after the Fukushima Dai-ichi Nuclear Power Plant (FDNPP) accident are strongly sorbed by fine particles, and they are therefore likely to be redistributed by hydro-sedimentary processes across catchments. Although regrettable, the Fukushima catastrophe and the associated massive radionuclide release provide a unique opportunity to track the dispersion of sediment in catchments exposed to typhoons and to better understand the anthropogenic impacts on particle-borne transfers within the natural environment. Fieldwork around FDNPP and subsequent lab work on Fukushima samples required the compliance with very demanding radioprotection and security rules. Here, we collected exposed riverbed sediment (n=162) along rivers and in reservoirs draining the catchments contaminated by the main radioactive pollution plume that extends across Fukushima Prefecture in November 2011, April 2012 and November 2012. We measured their gamma-emitting radionuclide activities and compared them to the documented surveys in nearby soils. We show that the ^{110m}Ag:^{137}Cs ratio provided a tracer of the dispersion of contaminated sediment in one specific catchment draining the most contaminated area. Our results demonstrate that the system was very reactive to the succession of summer typhoons and spring snowmelt. We identified a partial export of contaminated sediment from inland mountain ranges – exposed initially to the highest radionuclide fallout – to the coastal plains as soon as in November 2011, after a series of violent typhoons. This export was amplified by the spring snowmelt, and remaining contaminated material temporarily stored in the river channel was flushed by the typhoons that occurred during summer in 2012. This catchment behaviour characterized by the

high transmissivity of paddy fields strongly connected to the river network in upland mountain ranges and the potential storage in the coastal plains that are successively filled with contaminated sediment and then flushed was illustrated by the calculation of an index of hydro-sedimentary connectivity and the construction of river longitudinal profiles. We thereby suggest that coastal rivers have become a perennial supply of contaminated sediment to the Pacific Ocean. Our findings show that Fukushima accident produced original tracers to monitor particle-borne transfers across the affected area shortly after the catastrophe. Furthermore, we outlined that this accident generated a distinct geological record that will be useful for sediment dating behind reservoirs in Japan during the next decades.

1. INTRODUCTION

As a consequence of the magnitude 9.0 earthquake and the subsequent tsunami that occurred on 11 March 2011 (Simons et al., 2011), the Fukushima Dai-ichi Nuclear Power Plant (FDNPP) underwent a series of serious damages (Burns et al., 2012). After failure of the cooling systems, several hydrogen explosions affected three of the six nuclear reactors of the power plant on March 12, 14 and 15, and affected a fourth reactor which had already been stopped (Achim et al., 2012). Significant quantities of radionuclides were released into the environment between 12 and 31 March (Morino et al., 2013). Radioactive substance quantities released by the FDNPP accident were estimated to reach 11–40% (190-700 PBq) of the total amount of ^{131}I and 14–62% (12– 53.1 PBq) of the total ^{137}Cs emitted by Chernobyl accident (Chino et al., 2011; Nuclear Safety Commission of Japan, 2011; IRSN, 2012; Stohl et al., 2012; Winiarek et al., 2012). Despite the bulk of radionuclides (~80%) were transported offshore and out over the Pacific Ocean (Buesseler et al., 2011; Masson et al., 2011), significant wet and dry deposits of those

radionuclides occurred predominantly in Fukushima Prefecture on 15–16 March, leading to a strong contamination of soils (Yasunari et al., 2011; Kinoshita et al., 2011). In particular, 6.4 PBq of ^{137}Cs (~20% of the total emissions) were modeled to have deposited on Japanese soils (Stohl et al., 2012) over a distance of 70 km to the northwest of FDNPP (Fig. 1a). Soils characterized by a ^{137}Cs contamination exceeding 100 $kBq.m^{-2}$ cover ca. 3000 km² (MEXT, 2011).

When reaching such high levels, radioactive contamination constitutes a real threat for the local populations. Resulting radiations lead to an external exposure threat that depends on the spatial distribution of radionuclides and the time of exposition (Endo et al., 2012; Garnier-Laplace et al., 2011). This threat, associated with the possibility of transfer of contamination to plants, animals and direct ingestion of contaminated particles, will affect human activities such as agriculture, forest exploitation and fishing for long periods of time, depending on the half-life of the radionuclides (e.g., 2 yrs for ^{134}Cs; 30 yrs for ^{137}Cs). Those latter substances are strongly sorbed by soil particles (and especially by their clay, silt and organic matter fractions) and may therefore be delivered to rivers by runoff and erosion processes triggered on hillslopes (Motha et al., 2002; Tamura, 1964; Whitehead, 1978). This sediment may then further convey contaminants in rivers, and its transfer can lead to the dispersion of radioactive contamination across larger areas over time (Rogowski and Tamura, 1965, Simpson et al., 1976). To our knowledge, those transfers following the FDNPP releases have only been investigated at the scale of individual fields (e.g. Koarashi et al., 2012) or in very small catchments of northeastern Japan (Ueda et al., 2013). Still, assessing as soon as possible the spatial and temporal variations of radioactive contaminant dispersion has become one of the major concerns for the protection of natural ecosystems and human populations living in this region.

In addition to problems associated with the high radioactive contamination which justifies its urgent monitoring at the regional scale, this event, although regrettable, also constitutes a unique scientific opportunity to track in an original way particle-borne transfers that play a major role in global biogeochemical cycles (Van Oost et al., 2007) and in the transfer of contaminants within the natural environment (Meybeck, 2003). Conducting this type of study is particularly worthwhile in Japanese mountainous river systems exposed to both summer typhoons and spring snowmelt, where we can expect that those transfers are rapid, massive and episodic (Mouri et al., 2011).

During this study, fieldwork required being continuously adapted to the evolution of the delineation of restricted areas around FDNPP, and laboratory experiments on Fukushima samples necessitated the compliance with specific radioprotection rules (i.e., procedures for sample preparation, analysis and storage). In addition, the earthquake and the subsequent tsunami led to the destruction of river gauging stations in the coastal plains, and background data (discharge and suspended sediment concentrations) were unavailable during the study period. Monitoring stations have only become operational again from December 2012 onwards.

In this post-accidental context, this paper aims to provide alternative methods to estimate the early dispersion of contaminated sediment during the 20 months that followed the nuclear accident in those mountainous catchments exposed to a succession of erosive rainfall, snowfall and snowmelt events. It will also investigate, based on the radioisotopes identified, whether the accident produced geological records, i.e. characteristic properties in sediment deposit layers, that may be used in the future for sediment tracing and dating.

2. MATERIALS AND METHODS

2.1. Study site and mapping of initial soil contamination

The objective of the study that covered the period from November 2011 to November 2012 was to document the type and the magnitude of radioactive contamination found in sediment collected along rivers draining the main radioactive pollution plume that extends over 20 to 50 km to the northwest of FDNPP in Fukushima Prefecture (Fig. 1a). For this purpose, we measured their gamma-emitting radionuclide activities and compared them to the documented surveys in nearby soils. In association with the U.S. Department of Energy (DOE), the Japanese Ministry of Education, Culture, Sports, Science and Technology (MEXT) performed a series of detailed airborne surveys of air dose rates 1-m above soils and of radioactive substance deposition (gamma-emitting) in the ground surface shortly after the nuclear accident (from 6 to 29 April 2011) in Fukushima Prefecture (MEXT and DOE, 2011). The MEXT sampled and analysed gamma-emitting radionuclides in the upper 5-cm layer of soil collected from 2200 sites located within a radius of approximately 100 km around FDNPP during June and July 2011 to validate and enlarge the use of these airborne surveys (MEXT, 2011a). Background maps of point-based radionuclide inventories in soils (^{134}Cs + ^{137}Cs, ^{110m}Ag) designed in this study (Fig. 1a, 2, 3, 4, 7) were drawn from data provided by MEXT for these 2200 investigated locations. We hypothesised that those radionuclides were concentrated in the soil upper 2 cm layer, and that soils had a mean bulk density of 1.15 $g.cm^{-3}$ based on data collected in the area (Kato et al., 2011; Matsunaga et al., 2013). Within this set of 2200 soil samples, ^{110m}Ag activities were only reported for a selection of 345 samples that were counted long enough to detect this radioisotope (Fig. 3, 4). All activities were decay corrected to 14 June 2011. A map of total radiocaesium activities was interpolated across the entire study area by performing ordinary kriging to

appreciate regional fallout patterns in soils (Fig. 1a, 2, 7; Chilès and Delfiner, 1988; Goovaerts, 1997). A cross validation was then applied to the original data to corroborate the variogram model. The mean error (R) was defined as follows (Eq. 1):

$$R = \frac{1}{n}\sum_{i=1}^{n}\left[z^*(x_i) - z(x_i)\right], \qquad (1)$$

where $z^*(x_i)$ is the estimated value at x_i, and $z(x_i)$ is the measured value at x_i.

The ratio of the mean squared error to the kriging variance was calculated as described in Eq. (2):

$$S_R^2 = \frac{1}{n}\sum_{i=1}^{n}\left[z^*(x_i) - z(x_i)\right]^2 / \sigma_k^2(x_i), \quad (2)$$

where $\sigma^2 k(x_i)$ is the theoretical estimation variance for the prediction of $z^*(x_i)$.

The temporal evolution of contamination in rivers draining the main radioactive plume was analyzed based on samples (described in section 2.2) taken after the main erosive events which were expected to affect this area (i.e., the summer typhoons and the spring snowmelt). During the first fieldwork campaign in November 2011, we travelled through the entire area where access was unrestricted (i.e., outside the area of 20-km radius centered on FDNPP; Fig. 1b) and that potentially drained the main radioactive plume of Fukushima Prefecture, i.e. the Abukuma River basin (5200 km²), and the coastal catchments (Mano, Nitta and Ota Rivers, covering a total area of 525 km²). Those systems drain to the Pacific Ocean from an upstream altitude of 1835 m a.s.l. Woodland (79%) and cropland (18%) represent the main land uses in the area. Mean annual precipitation varies appreciably across the study area (1100–2000 mm), in

response to the high variation of altitude and relief and the associated variable importance of snowfall.

During the second campaign (April 2012), based on the results of the first survey, the size and the delineation of the study area were adapted for a set of practical, logistical and safety reasons. Therefore, we targeted our sampling on the coastal catchments, where contamination was the highest and where the application of the potential tracer that we identified was the most promising.

2.2. Sample collection

We collected representative river sediment samples at exposed subaerial sites free of vegetation on channel bars between 17 and 23 November 2011 (69 sampling sites), between 3 and 8 April 2012 (40 sampling sites) and between 8 and 12 November 2012 (53 sampling sites) along the main rivers draining the area and some of their major tributaries. At each sampling site, five to ten subsamples of fine sediment that is likely to be deposited after the last major flood were collected at several locations selected randomly down to the underlying coarser cobble or gravel layer across a 10-m² surface by the means of a plastic trowel. They were subsequently used to prepare a composite sample representative of the fine sediment deposited on the channel bars. Bulk samples were dried, weighed, ground to a fine powder, packed into 15 ml pre-tared polyethylene specimen cups and sealed airtight. During the November 2012 fieldwork campaign, we also had the opportunity to collect samples of the different layers representative of the 1.6-m deep sediment sequence that accumulated behind Yokokawa dam on Ota River.

2.3. Radionuclide analyses

Radionuclide activities (^{134}Cs, ^{137}Cs, ^{110m}Ag) in all samples were determined by gamma spectrometry using very low-background coaxial N- and P-types HPGe detectors with a relative efficiency of ca. 50% at 1332 keV. Counting time of soil and sediment samples varied between 8×10^4 and 200×10^4 s to allow the detection of ^{110m}Ag, which was present in much lower activities in the samples (2–2390 Bq kg^{-1}) than ^{134}Cs and ^{137}Cs (500–1,245,000 Bq kg^{-1}). The ^{137}Cs activities were measured at the 661 keV emission peak. The ^{134}Cs activities were calculated as the mean of activities derived from measurements conducted at 604 keV and 795 keV (^{228}Ac activities being negligible compared to ^{134}Cs activities) as both peaks are associated with the largest gamma emission intensities of this radionuclide. The presence of ^{110m}Ag was confirmed by the detection of emission peaks at 885, 937 and 1384 keV, but activities were calculated from results obtained at 885 keV only. Minimum detectable activities in ^{110m}Ag for 24h count times reached 2 Bq.kg^{-1}. Errors reached ca. 5% on ^{134}Cs and ^{137}Cs activities, and 10% on ^{110m}Ag activities at the 95% confidence level. All measured counts were corrected for background levels measured at least every 2 months as well as for detector and geometry efficiencies. Results were systematically expressed in Bq.kg^{-1} of dry weight. Counting efficiencies and quality assurance were conducted using internal and certified International Atomic Energy Agency (IAEA) reference materials prepared in the same specimen cups as the samples. All radionuclide activities were decay corrected to the date of 14 June 2011 corresponding to the reference date of the MEXT soil sampling campaign (used to compute the background contamination maps; see section 2.1 for details) that was conducted just before the occurrence of typhoons in 2011 (July–September).

2.4. Calculation of a hillslope-to-sink hydro-sedimentary connectivity index

A connectivity index was computed according to the method developed by Borselli et al. (2008) to outline the spatial linkages and the potential connection between the sediment eroded from hillslopes by runoff processes and the different storage areas identified within catchments. These areas may either store sediment temporarily (i.e., reservoirs, lakes or local depressions in the floodplain) or definitively (i.e., outlets). Considering the lack of specific-event data such as soil erosion rates, discharge and suspended sediment concentrations, this index of connectivity based on GIS data tended to describe the general hydro-sedimentary behaviour of the investigated catchments. To calculate this index, landscape morphological characteristics and recent land use patterns were derived from high resolution databases. The potential of various land use surfaces to produce or store sediment was also assessed.

The calculation was conducted on a Digital Elevation Model (DEM) with a 10-m regular grid provided by the Geospatial Information Authority of Japan (GSI) from the Ministry of Land, Infrastructure, Transport and Tourism (http://www.gsi.go.jp/). This DEM was computed by the GSI from data obtained by LIDAR airborne monitoring surveys.

Values of the weighting cropping and management parameter (the so-called 'C-factor'), originally used in the USLE equation (USDA, 1978), were determined based on data found in the literature (Borselli et al., 2008; Kitahara et al., 2000; Yoshikawa et al., 2004) and applied to the different land use classes observed in the catchments and determined by a multitemporal and multispectral classification of SPOT-4 and SPOT-5 satellite images. SPOT-4 20-m resolution images dated from May 5, June 3 and September 10 2010, and SPOT-5 10-m resolution images dated from March 18, April 13 and 24, 2011. Differences in spectral responses (reflectances) between land uses allowed their spatial discrimination using ENVI 4.8 software. Then, based on their respective vegetal cover density during the spring season and their implications on soil

sensitivity to erosion, three main land uses were identified (i.e., forests, croplands and built-up areas). Additionally, surface water areas (i.e., rivers, lakes, reservoirs) were delineated. The land use map was validated by generating a set (n=150) of random points on the map and by comparing the classification output with the land use determined visually on available aerial photographs of the study area.

Hydrological drainage networks were derived from the GSI 10-m regular grid DEM using hydrologic analysis tools available from ArcGIS10 (ESRI, 2011). As several sections of hydrological networks did not coincide with the observed ones due to anthropogenic modifications introduced for urban and rural landscape management, manual corrections were applied, based on the analysis of the SPOT-4, SPOT-5 images and maps provided by the ArcGIS Online Map and Geoservices (ESRI, 2013).

3. RESULTS AND DISCUSSION

3.1. Contamination of soils and river sediments

The map of total cesium activities in soils of the study area was drawn by performing ordinary kriging on the MEXT soil database (Fig. 1a, 2, 7). A pure nugget (sill=1.07*10^9Bq².kg^{-2}) and a Gaussian model (Anisotropy=357°, Major range=69,100m, Minor range=65,000m and Partial sill=1.76*10^9 Bq².kg^{-2}) were nested into the experimental variogram (Fig. S1). This high nugget value may be influenced by the limited spacing between MEXT sampling locations (ca. 200 m) that did not allow to assess the very close-range spatial dependence of the data, and by the impact of vegetation cover variations on initial fallout interception. Nevertheless, the resulting initial soil contamination map was considered to be relevant, as the mean error was close to zero

(-1.19Bq.kg^{-1}) and the ratio of the mean squared error to the kriging variance remained close to unity (0.99).

Eight months after the accident, main anthropogenic gamma-emitting radionuclides detected in river sediment across the area were ^{134}Cs, ^{137}Cs and ^{110m}Ag. Trace levels in ^{110m}Ag ($t_{1/2}$ = 250 d) were previously measured in soils collected near the power plants (Tagami et al., 2011; Shozugawa et al., 2012) as well as in zooplankton collected off Japan in June 2011 (Buesseler et al., 2012), but a set of systematic ^{110m}Ag measurements conducted at the scale of entire catchments had not been provided so far. This anthropogenic radioisotope is a fission product derived from ^{235}U, ^{238}U or ^{239}Pu (JAEA, 2010). It is considered to have a moderate radiotoxicity as it was shown to accumulate in certain tissues such as in liver and brain of sheep and pig (Oughton, 1989; Handl et al., 2000). This radioisotope was observed shortly after Chernobyl accident but, in this latter context, it was rather considered as an activation product generated by corrosion of silver coating of primary circuit components and by erosion of fuel rod coatings containing cadmium (Jones et al., 1986). The presence of ^{125}Sb ($t_{1/2}$ = 2.7 y), which is also a fission product, was also detected in most samples (1-585 Bq.kg^{-1}; data not shown). All other short-lived isotopes (e.g., ^{131}I [$t_{1/2}$ = 8 d], ^{136}Cs [$t_{1/2}$ = 13 d], ^{129m}Te [$t_{1/2}$ = 34 d]) that were found shortly after the accident in the environment were not detected anymore in the collected sediment samples (Shozugawa et al., 2012). By November 2011, $^{134+137}$Cs activities measured in river sediment ranged between 500–1,245,000 Bq kg^{-1}, sometimes far exceeding (by a factor 2 to 20) the activity associated with the initial deposits on nearby soils (Fig. 2). This result confirms the concentration of radionuclides in fine river sediments because of their strong particle-reactive behaviour (Tamura, 1964; Whitehead, 1978; Motha et al., 2002).

Those contamination levels are between 1 and 5 orders of magnitude higher than before the accident (Fukuyama et al., 2010). As we could expect it, the highest contamination levels (total $^{134+137}$Cs activities exceeding 100,000 Bq. kg^{-1}) were measured in sediment collected along the coastal rivers (i.e., Mano and Nitta Rivers) draining the main radioactive plume (Fig. 2). Contamination levels were logically much lower in sediment collected along the Abukuma River that drains less contaminated areas. The analyses conducted by the Japanese Ministry of Environment (MoE) provided an additional temporal insight into contaminated sediment exports in this area. Our samples were collected in November 2011, whereas samples provided by MoE showed that contamination of sediment was systematically the highest in material collected in September 2011. The presence of contamination hotspots close to Fukushima City and behind a large dam located upstream of the city is likely due to the rapid wash-off of radionuclides on urban surfaces during the first series of rainfall events that followed the accident, to their concentration in urban sewers systems (Urso et al., 2013) and their subsequent export to the rivers. This rapid export of radionuclides shortly after the accident along the Abukuma River is confirmed by data collected by the MoE (Fig. 2) showing a peak of contamination in sediment collected in September 2011, and then a huge decrease to low activities even during snowmelt. Along the Hirose River, the snowmelt (in March 2012) led in contrast to an increase in sediment contamination.

At the light of those first results outlining a very rapid wash-off of radionuclides obtained following the accident in the Abukuma River basin, we decided to focus the next fieldwork campaigns on the coastal basins where radionuclide activities in sediment were the highest. We extended sampling to the Ota River catchment, closer to FDNPP, where access was unauthorized during the first campaign (Fig. 1b).

3.2. Dispersion of radioactive sediment along river channels

Whilst ^{137}Cs and ^{134}Cs gamma-emitting radioisotopes constitute by far the most problematic contaminants (with total activities in soils ranging from 50 to 1,110,000 $Bq.kg^{-1}$), ^{110m}Ag was also identified and measured in most samples (with activities ranging from 1 to 3150 $Bq.kg^{-1}$). Because of these low activities, contribution of ^{110m}Ag to the global dose rates was considered to be negligible. It appeared from the analysis of the MEXT soil database that the initial fallout pattern of ^{110m}Ag displayed significant spatial variations that were not observed for the radiocaesium fallout pattern at the scale of the entire Fukushima Prefecture. Soil activities in ^{110m}Ag were the highest within the main radiocaesium contamination plume as well as at several places along the coast located between 40 and 50 km to the north of the power plant (MEXT, 2011b).

Most interestingly, the 345 values of ^{110m}Ag:^{137}Cs ratio in MEXT soil samples strongly varied across the entire region (0.0004–0.15 with a mean of 0.006; Fig. 4), whereas the 2200 values of ^{134}Cs:^{137}Cs ratio remained relatively stable across the contamination plume (0.4–1.5 with a mean value close to 0.9; data not shown). Fallout patterns of ^{110m}Ag:^{137}Cs ratio in soils of Fukushima Prefecture provided a way to delineate three distinctive zones (Fig. 3, Table 1; i.e., ‘eastern’, ‘southern’ and ‘western’ zones). A Kruskal–Wallis H-test was conducted and it confirmed that these three zones were characterized by significantly different values of ^{110m}Ag:^{137}Cs ratio ($P < 0.001$; $\alpha = 0.05$).

The differences in fallout patterns between ^{110m}Ag and ^{137}Cs were most likely due to the fact that those radionuclides were released during different explosions affecting reactors containing different fuel assemblages (Schwantes et al., 2012). Furthermore, even though the

overall chronology of the reactor explosions could be reconstructed (e.g., Le Petit et al., 2012), the subsequent radionuclide deposits are still imperfectly understood. To our knowledge, studies that modeled radionuclide deposits across Fukushima Prefecture dealt with ^{131}I and/or ^{137}Cs exclusively (e.g., Morino et al., 2013), and never with ^{110m}Ag. The single main operational difference between the FDNPP damaged reactors is that mixed-oxide (MOX) containing plutonium fuel that generates ^{110m}Ag as a fission product was only used in reactor 3 (Le Petit et al., 2012), which may explain this different radionuclide deposition pattern.

In the coastal study area, the area covered by both 'western' and 'eastern' zones was unfortunately only large enough in the Nitta River catchment to be subsequently used to track the dispersion of contaminated sediment based on values of this ratio measured in soils as well as in river sediment (the area covered by the 'western' zone was too small in the Mano River catchment, and no soil sample was collected by MEXT in the 'western' part of the Ota River catchment; Fig.4). Descriptive statistics of ^{110m}Ag:^{137}Cs values in the single Nitta catchment confirmed that the spatial variability of this ratio provided significantly different signatures in both 'western' and 'eastern' areas in this catchment (Table 2).

In order to use this ratio to track sediment pathways, both radionuclides should exhibit a similar behaviour in soils and sediment. A wide range of investigations dealt with ^{137}Cs behaviour in soils, but a much lower number of studies addressed the behaviour of ^{110m}Ag in soils and sediment. However, according to our literature review, ^{137}Cs and ^{110m}Ag are characterized by similar solid/liquid partition coefficient (K_d) values ($9.0*10^1$-$4.4*10^3$) in both soils and sediment (IAEA, 1994; IPSN, 1994; Garnier-Laplace et al., 1997; Roussel-Debet and Colle, 2005). Furthermore, it was demonstrated that ^{110m}Ag is not mobile in soils (Alloway, 1995) and that it tends to concentrate in the few first centimeters of the soil uppermost surface, as

it was reported for ^{137}Cs in Fukushima region (Kato et al., 2012; Handl et al., 2000; Shang and Leung, 2003). Those literature data validate the relevance of using this ratio to discriminate between sediment eroded from the mountain ranges located in the main contamination plume vs. sediment mobilized from the coastal plains. This investigation is particularly crucial in the case of coastal rivers in Fukushima Prefecture to guide the implementation of appropriate soil and river management measures. Nitta River drains mountainous areas characterized by a high initial contamination to the Pacific Ocean, by flowing across coastal plains that were relatively spared by initial continental fallout but that are still currently densely populated (e.g. in Minamisoma town).

The relative contribution of each source in the composition of riverbed sediment collected during the three sampling campaigns in the Nitta catchment was then quantified through the application of a binary mixing model. As an example, the relative contribution of 'western' source area X_w was determined from Eq. (3):

$$X_W = \frac{(\frac{^{110m}Ag}{^{137}Cs})_S - (\frac{^{110m}Ag}{^{137}Cs})_E}{(\frac{^{110m}Ag}{^{137}Cs})_W - (\frac{^{110m}Ag}{^{137}Cs})_E} * 100 , \quad (3)$$

Where X_W is the percentage fraction of the western source area, $(^{110m}Ag{:}^{137}Cs)_W$ and $(^{110m}Ag{:}^{137}Cs)_E$ are the median values of $^{110m}Ag{:}^{137}Cs$ ratio measured in MEXT soil samples collected in the 'western' and the 'eastern' source areas of the Nitta catchment, i.e. 0.0024 and 0.0057 respectively (Table 2), and $(^{110m}Ag{:}^{137}Cs)_S$ is the isotopic ratio measured in the river sediment sample. We did not include initial river sediment as a third end-member as the violent typhoons that occurred between the accident (March 2011) and our first fieldwork campaign (November

2011) likely flushed the fine riverbed sediment that was already present in the channels before the accident.

Application of the mixing model illustrates the very strong reactivity of this catchment and the entire flush of sediment stored in the river network during a one-year period only (Fig. 5). In November 2011, following the summer typhoons (i.e., Man-On on 20 July and Roke on 22 September that generated cumulative precipitation that reached between 215–310 mm across the study area), contaminated soil was eroded from upstream fields and supplied to the upstream sections of the rivers (Fig. 5a). Then, this sediment was exported to the coastal plains during the discharge increase generated by the snowmelt in March 2012, as illustrated by the measurements conducted on material sampled in April 2012 (Fig. 5b). Finally, sediment deposited within the river network was flushed by the typhoons that occurred during summer in 2012. Those typhoons were less violent than the ones that happened in 2011, and led to less intense erosion than during the previous year, but they were sufficiently powerful to increase river discharges, to export the sediment stored in the river channel and to replace it with material originating from closer areas (Fig. 5c).

This massive transfer of contaminated sediment reflects the strong seasonality of sediment fluxes in these rivers affected by both typhoons and spring snowmelt. Our results confirm that, by exporting contaminated particles originating from the main inland radioactive plume, coastal rivers are likely to have become a significant and perennial source of radionuclide contaminants to the Pacific Ocean off Fukushima Prefecture. This could at least partly explain the still elevated radionuclide levels measured in fish off Fukushima Prefecture (Buesseler et al., 2012).

Quantification of the hydro-sedimentary connectivity between hillslopes and the identified sinks in the three coastal catchments provided additional information on the timing of sediment transfer processes and their preferential pathways observed along the investigated rivers (Fig. 6). Paddy fields located in the upstream part of both Nitta and Mano River catchments were well connected to the thalweg and they constituted therefore an important supply of contaminated material to the rivers or to small depressions located in the floodplain. In contrast, in the flat coastal plains of those catchments, large cultivated surfaces were poorly connected to the rivers. A distinct situation was observed in the Ota River catchment. In the upper part of this catchment, land use is dominated by forests that are much less erodible than cropland, but that could deliver contaminated material to the river during heavy rainfall (Fukuyama et al., 2010). Furthermore, the high slope gradients observed in this area may have led to the more frequent occurrence of mass movements in this area. This contaminated material was then stored in the large Yokokawa reservoir. In the downstream part of the Ota River catchment, paddy fields located in the vicinity of rivers were well connected to the watercourses which contrasts with the situation outlined in the coastal plains of the Mano and Nitta River catchments.

This transfer timing and preferential pathways are confirmed when we plot the contamination in total $^{134+137}$Cs measured in sediment collected during the three fieldwork campaigns along the longitudinal profiles of the investigated rivers (Fig. 7). Overall, we observed a general decrease in the contamination levels measured between the first and the last campaign, especially in the Nitta River catchment (Fig. 7, left panels) where the difference is particularly spectacular along the upstream sections of the Nitta (Fig. 7; profile c-d) and Iitoi Rivers (Fig. 7; profile g-e). Our successive measurements suggest that there has been a

progressive flush of contaminated sediment towards the Pacific Ocean. However, the mountain range piedmont and the coastal plains that have remained continuously inhabited constitute a potentially large buffer area that may store temporarily large quantities of radioactive contaminants from upstream areas. However, our data and the drawing of the longitudinal profiles suggest that this storage was of short duration in the river channels. A similar flush was observed between November 2011 and November 2012 along both Mano and Ota Rivers (Fig. 7; profiles a-b and i-j). They are equipped with dams at 20 km from the outlet for Nitta River, and at 16 and 12 km from the outlet for the Ota river. Only the finest – and most contaminated – material is exported from their reservoirs, as suggested by the very high $^{134+137}$Cs activities measured in sediment collected just downstream of the dams (Fig. 7; profiles a-b and i-j). Those reservoirs stored very large quantities of contaminated sediment, as illustrated by the contamination profile documented in sediment accumulated behind Tetsuzen dam (Fig. 8). Identification of a 10-cm sediment layer strongly enriched in $^{134+137}$Cs (308,000 Bq.kg^{-1}) and overlaid by a more recent and less contaminated layer (120,000 Bq.kg^{-1}) shows that Fukushima accident produced a distinct geological record that will be useful for sediment dating and estimation of stocks of contaminated material in this region of Japan during the next years and decades.

4. Conclusions

The succession of typhoons and snowmelt events during the 20 months that followed FDNPP accident led to the rapid and massive dispersion of contaminated sediment along coastal rivers draining the catchments located in the main radioactive pollution plume. In this unique post-

accidental context, the absence of continuous river monitoring has necessitated the combination of indirect approaches (mapping and tracing based on radioisotopic ratios, connectivity assessment) to provide this first overall picture of early sediment dispersion in Fukushima coastal catchments. These results obtained on riverbed sediment should be compared to the measurements conducted on suspended sediment that are being collected since December 2012. The combination of those measurements with discharge and suspended sediment concentration data will also allow calculating exports of contaminated sediment to the Pacific Ocean. Our results showing the rapid dispersion of contaminated sediment from inland mountain ranges along the coastal river network should also be compared to the ones obtained with the conventional fingerprinting technique based on the geochemical signatures of contrasted lithologies. Fukushima coastal catchments investigated by this study are indeed constituted of contrasted sources (volcanic, plutonic and metamorphic sources in upper parts vs. sedimentary sources in the coastal plains). This unique combination of surveys and techniques will provide very important insights into the dispersion of particle-borne contamination in mountainous catchments that are particularly crucial in this post-accidental context, but that will also be applicable in other catchments of the world where other particle-borne contaminants are problematic.

ACKNOWLEDGMENTS

This work is a part of the TOFU (*Tracing the environmental consequences of the Tohoku earthquake-triggered tsunami and Fukushima accident*) project, funded by the joint French National Research Agency-Flash Japon (ANR- 11-JAPN-001) and Japan Science and Technology agency/J-RAPID programme. Support and data provided by the Japanese Ministry of Environment (http://www.env.go.jp/en/) were greatly appreciated. LSCE (Laboratoire des Sciences du Climat et de l'Environnement) contribution No.X. SPOT-Image and the French national CNES-ISIS (Centre National d'Etudes Spatiales – Incentive for the Scientific use of Images from the SPOT system) program are also acknowledged for providing the SPOT data.

REFERENCES

Achim, P., Monfort, M., Le Petit, G., Gross, P., Douysset, G., Taffary, T., Blanchard, X., Moulin, C., 2012. Analysis of radionuclide releases from the Fukushima Dai-ichi Nuclear Power Plant accident – Part II. *Pure and Applied Geophysics*. DOI 10.1007/s00024-012-0578-1.

Alloway, B. J, Ed., 1995. *Heavy Metals in Soils*, 2nd ed.; Blackie Academic and Professional.

Borselli, L., Cassi, P., Torri, D., 2008. Prolegomena to sediment and flow connectivity in the landscape: A GIS and field numerical assessment. *Catena* 75, 268-277.

Buesseler, K., Aoyama, M., Fukasawa, M., 2011. Impacts of the Fukushima nuclear power plants on marine radioactivity. *Environ. Sci. Technol.* 45, 9931-9935.

Buesseler, K. O., 2012. Fishing for answers off Fukushima. *Science* 338, 480-482.

Buesseler, K.O., Jayne, S.R., Fisher, N.S., Rypina, I.I., Baumann, H., Baumann, Z., Breiera, C.F., Douglass, E.M., George, J., Macdonald, A.M., Miyamoto, H., Nishikawa, J., Pike, S.M., Yoshida, S., 2012. Fukushima-derived radionuclides in the ocean and biota off Japan. *Proc. Natl. Acad. Sci. USA* 109, 5984-5988.

Burns, P.C., Ewing, R.C., Navrotsky, A., 2012. Nuclear fuel in a reactor accident. *Science* 335, 1184-1188.

Chilès, J.P.; Delfiner, P., 1988. *Geostatistics: Modeling Spatial Uncertainty;* Wiley: New York.

Chino, M., Nakayama, H., Nagai, H., Terada, H., Katata, G., Yamazawa, H., 2011. Preliminary estimation of release amounts of ^{131}I and ^{137}Cs accidentally discharged from the Fukushima Daiichi nuclear power plant into the atmosphere. *J. Nucl. Sci. Technol.* 48, 1129-1134.

Endo, S., Kimura, S., Takatsuji, T., Nanasawa, K.,Imanaka, T., Shizuma, K., 2012. Measurement of soil contamination by radionuclides due to the Fukushima Dai-ichi Nuclear Power Plant accident and associated estimated cumulative external dose estimation. *J. Environ. Radioact.* 111, 18-27.

ESRI, 2011. ArcGIS Desktop: Release 10. Redlands, CA: Environmental Systems Research Institute.

ESRI, 2013. ArcGIS Online Map and Geoservices. http://www.esri.com/software/arcgis/arcgis-online-map-and-geoservices/map-services

Fukuyama, T., Onda, Y., Gomi, T., Yamamoto, K., Kondo, N., Miyata, S., Kosugi, K., Mizugaki, S., Tsubonuma, N., 2010. Quantifying the impact of forest management practice on the runoff of the surface-derived suspended sediment using fallout radionuclides. *Hydrol. Process. 24*, 596-607.

Garnier-Laplace, J., Fournier-Bidoz, V., Baudin, J., 1997. État des connaissances sur les échanges entre l'eau, les matières en suspension et les sédiments des principaux radionucléides rejetés par les centrales nucléaires en eau douce. *Radioprotection* 3 (1), 49-71.

Garnier-Laplace, J., Beaugelin-Seiller, K., Hinton, T.G., 2011. Fukushima wildlife dose reconstruction signals ecological consequences. *Environ. Sci. Technol.* 45, 5077-5078.

Goovaerts, P., 1997. *Geostatistics For Natural Resources Evaluation*; Oxford Univ. Press: Oxford, U.K.

Handl, J., Kallweit, E., Henning, M., Szwec, L., 2000. On the long-term behaviour of ^{110m}Ag in the soil–plant system and its transfer from feed to pig. *J. Environ. Radioact.* 48 (2), 159-170.

IAEA, 1994. *Handbook of Parameter Values for the Prediction of Radionuclide Transfer in the Terrestrial and Freshwater Environment*; IAEA Technical Report series TRS-364. International Atomic Energy Agency, Vienna. http://www-pub.iaea.org/MTCD/publications/PDF/trs472_web.pdf.

IPSN, 1994. *Etudes bibliographiques sur les échanges entre l'eau les matières en suspension et les sédiments des principaux radionucléides rejetés par les centrales nucléaires*; Rapport IPSN, SERE 94/073; Institut de Protection et de Sûreté Nucléaire : Cadarache.

Institut de Radioprotection et de Sûreté Nucléaire (IRSN), 2012. Bilan des conséquences de l'accident de Fukushima sur l'environnement au Japon, un an après l'accident (28/02/2012). http://www.irsn.fr/FR/base_de_connaissances/Installations_nucleaires/La_surete_Nucleaire/Les-accidents-nucleaires/accident-fukushima-2011/fukushima-1-an/Documents/IRSN_Fukushima_Synthese-Environnement_28022012.pdf.

Kato, H., Onda, Y., Teramage, M., 2012. Depth distribution of ^{137}Cs, ^{134}Cs, and ^{131}I in soil profile after Fukushima Dai-ichi Nuclear Power Plant Accident. *J. Environ. Radioact.* 111, 59-64.

Japanese Atomic Energy Agency (JAEA), 2010. Ag-110m – Nuclide Information. http://wwwndc.jaea.go.jp/cgi-bin/nuclinfo2010?47,110

Jones, G.D., Forsyth, P.D., Appleby, G.B., 1986. Observation of ^{110m}Ag in Chernobyl fallout. *Nature* 322, 313.

Kinoshita, N., Sueki, K., Sasa, K., Kitagawa, J., Ikarashi, S., Nishimura, T., Wong, Y.S., Satou, Y., Handa, K., Takahashi, T., Sato, M., Yamagata, T., 2011. Assessment of individual radionuclide distributions from the Fukushima nuclear accident covering central-east Japan. *Proc. Natl. Acad. Sci. USA* 108, 19526–19529.

Kitahara, H., okura, Y., Sammori, T., Kawamami, A., 2000. Application of Universal Soil Loss Equation (USLE) to Mountainous Forests in Japan. *Journal of Forest Research* 5, 231-236.

Koarashi, J., Atarashi-Andoh, M., Matsunaga, T., Sato, T., Nagao, S., Nagai, H., 2012. Factors affecting vertical distribution of Fukushima accident-derived radiocesium in soil under different land-use conditions. *Science of the Total Environment* 431, 392–401.

Le Petit, G., Douysset, G., Ducros, G., Gross, P., Achim, P., Monfort, M., Raymond, P., Pontillon, Y., Jutier, C., Blanchard, X., Taffary, T., Moulin, C., 2012. Analysis of Radionuclide Releases from the Fukushima Dai-Ichi Nuclear Power Plant Accident - Part I. *Pure and Applied Geophysics*. DOI 10.1007/s00024-012-0581-6.

Masson, O., et al., 2011. Tracking of airborne radionuclides from the damaged Fukushima Dai-ichi nuclear reactors by European networks. *Environ. Sci. Technol.* 45, 7670-7677.

Matsunaga, T., Koarashi, J., Atarashi-Andoh, M., Nagao, S., Sato, T., Nagai, H., 2013. Comparison of the vertical distributions of Fukushima nuclear accident radiocesium in soil before and after the first rainy season, with physicochemical and mineralogical interpretations. *Science of the Total Environment* 447, 301-314.

Meybeck, M., 2003. Global analysis of river systems: from Earth system controls to Anthropocene syndromes. *Phil. Trans. R. Soc. Lond. B* 358, 1935-1955.

Ministry of Education, Culture, Sports Science and Technology (MEXT), 2011a. Preparation of distribution map of radiation doses, etc. (Map of radioactive cesium concentration in soil) by MEXT. http://radioactivity.mext.go.jp/en/contents/5000/4165/24/1750_083014.pdf

Ministry of Education, Culture, Sports Science and Technology (MEXT), 2011b. Preparation of Distribution Map of Radiation Doses, etc. (Maps of Concentration of Tellurium 129m and Silver 110m in Soil) by MEXT.
http://radioactivity.mext.go.jp/en/contents/5000/4168/24/1750_1031e_2.pdf

Ministry of Education, Culture, Sports Science and Technology (MEXT) and U.S. Department of Energy (DOE) MEXT and DOE Airborne Monitoring, 2011. http://radioactivity.mext.go.jp/en/list/203/list-1.html

Morino, Y., Ohara, T., Watanabe, M., Hayashi, S., Nishizawa, M., 2013. Episode analysis of deposition of radiocesium from the Fukushima Daiichi nuclear power plant accident. *Environmental Science and Technology*. DOI 10.1021/es304620x.

Motha, J.A., Wallbrink, P.J., Hairsine, P.B., Grayson, R.B. , 2002. Tracer properties of eroded sediment and source material. *Hydrol. Process.*16, 1983– 2000.

Mouri, G., Shiiba, M., Hori, T., Oki, T., 2011. Modeling reservoir sedimentation associated with an extreme flood and sediment. *Geomorphology* 125, 263-270.

Nuclear Safety Commission of Japan (NSC), 2011. Trial estimation of emission of radioactive materials (^{131}I, ^{137}Cs) into the atmosphere from Fukushima Dai-ichi nuclear power station. http://www.nsc.go.jp/NSCenglish/geje/2011%200412%20press.pdf.

Oughton, D., 1989. The environmental chemistry of radiocaesium and other nuclides. PhD thesis, University of Manchester.

Rogowski, A.S., Tamura, T., 1965. Movement of ^{137}Cs by runoff, erosion and infiltration on the alluvial Captina silt loam. *Health Physics* 11(12), 1333-1340.

Roussel-Debet, S., Colle, C., 2005. Comportement de radionucléides (Cs, I, Sr, Se, Tc) dans le sol : proposition de valeurs de K_d par défaut. *Radioprotection 40* (2), 203-229.

Schwantes, J.M., Orton, C.R., Clark, R.A., 2012. Analysis of a nuclear accident: fission and activation product releases from the Fukushima Daiichi nuclear facility as remote indicators of source identification, extent of release, and state of damaged spent nuclear fuel. *Environ. Sci. Technol.* 46, 8621-8627.

Shang, Z.R.; Leung, J.K.C, 2003. ^{110m}Ag root and foliar uptake in vegetables and its migration in soil. *J. Environ. Radioact.* 65 (3), 297-307.

Shozugawa, T.; Nogawa, N.; Matsuo, M., 2012. Deposition of fission and activation products after the Fukushima Dai-ichi nuclear power plant accident. *J. Env. Pol.* 163, 243-247.

Simons, M., Minson, S.E., Sladen, A., Ortega, F., Jiang, J., Owen, S.E., Meng, L., Ampuero, J.P., Wei, S., Chu, R., Helmberger, D.V., Kanamori, H., Hetland, E., Moore, A.W., Webb, F.H., 2011. The 2011 Magnitude 9.0 Tohoku-Oki Earthquake: Mosaicking the Megathrust from Seconds to Centuries. *Science* 332, 1421-1425.

Simpson, H.J., Olsen, C.R., Trier, R.M., Williams, S.C, 1976. Man-made radionuclides and sedimentation in the Hudson River estuary. *Science* 194, 179-183.

Stohl, A., Seibert, P., Wotawa, G., Arnold, D. , Burkhart, J.F. , Eckhardt, S. , Tapia, C. , Vargas, A. , Yasunari, T.J., 2012. Xenon-133 and caesium-137 releases into the atmosphere from the Fukushima Dai-ichi nuclear power plant: determination of the source term, atmospheric dispersion, and deposition. *Atmos. Chem. Phys.* 12, 2313-2343.

Tagami, K., Uchida, S., Uchihori, Y., Ishii, N., Kitamura, H., Shirakawa, Y., 2011. Specific activity and activity ratios of radionuclides in soils collected about 20 km from the Fukushima Daiichi nuclear power plant: Radionuclide release to the south and southwest. *Sci. Total Environ.* 409, 4885-4888.

Tamura, T., 1964. Consequences of activity release: selective sorption reactions of cesium with soil minerals. *Nucl. Safety* 5, 262-268.

Ueda, S., Hasegawa, H., Kakiuchi, H., Akata, N., Ohtsuka, Y., Hisamatsu, S., 2013. Fluvial discharges of radiocaesium from watersheds contaminated by the Fukushima Dai-ichi Nuclear Power Plant accident, Japan. *Journal of Environmental Radioactivity* 118, 96-104.

Urso, L., Kaiser, J.C., Andersson, K.G., Andorfer, H., Angermair, G., Gusel, C., Tandler, R., 2013. Modeling of the fate of radionuclides in urban sewer systems after contamination due to nuclear or radiological incidents. *Journal of Environmental Radioactivity* 118, 121-127.

USDA, 1978. Predicting rainfall erosion losses; in A Guide to Conservation Planning. USDA Agriculture Handbook No.537, pp.58.

Van Oost, K., Quine, T.A., Govers, G., De Gryze, S., Six, J., Harden, J.W., Ritchie, J.C., McCarty, G.W., Heckrath, G., Kosmas, C., Giraldez, J.V., Marques da Silva, J.R., Merckx, R., 2007. The impact of agricultural soil erosion on the global carbon cycle. *Science* 318(5850), 626-629.

Whitehead, D.C., 1978. Iodine in soil profiles in relation to iron and aluminium oxides and organic matter. *J. Soil Sci.* 29, 88-94.

Winiarek, V., Bocquet, M., Saunier, O., Mathieu, A., 2012. Estimation of errors in the inverse modeling of accidental release of atmospheric pollutant: application to the reconstruction of the cesium-137 and iodine-131 source terms from the Fukushima Daiichi power plant. *J. Geophys. Res.* 117, D05122; DOI 10.1029/2011JD016932.

Yasunari, T.J., Stohl, A., Hayano, C., Burkhart, J.F., Eckhardt, S., Yasunari, T., 2011. Cesium-137 deposition and contamination of Japanese soils due to the Fukushima nuclear accident. *Proc. Natl. Acad. Sci. USA* 108, 19530-19534.

Yoshikawa, S., Yamamoto, H., Hanano, Y., Ishihara, A., 2004. Hilly-Land Soil Loss Equation (HSLE) for Evaluation of Soil Erosion Caused by the Abandonment of Agricultural Practices. *JARQ* 38, 21-29. http://www.jircas.affrc.go.jp.

Figure 1

Click here to download high resolution image

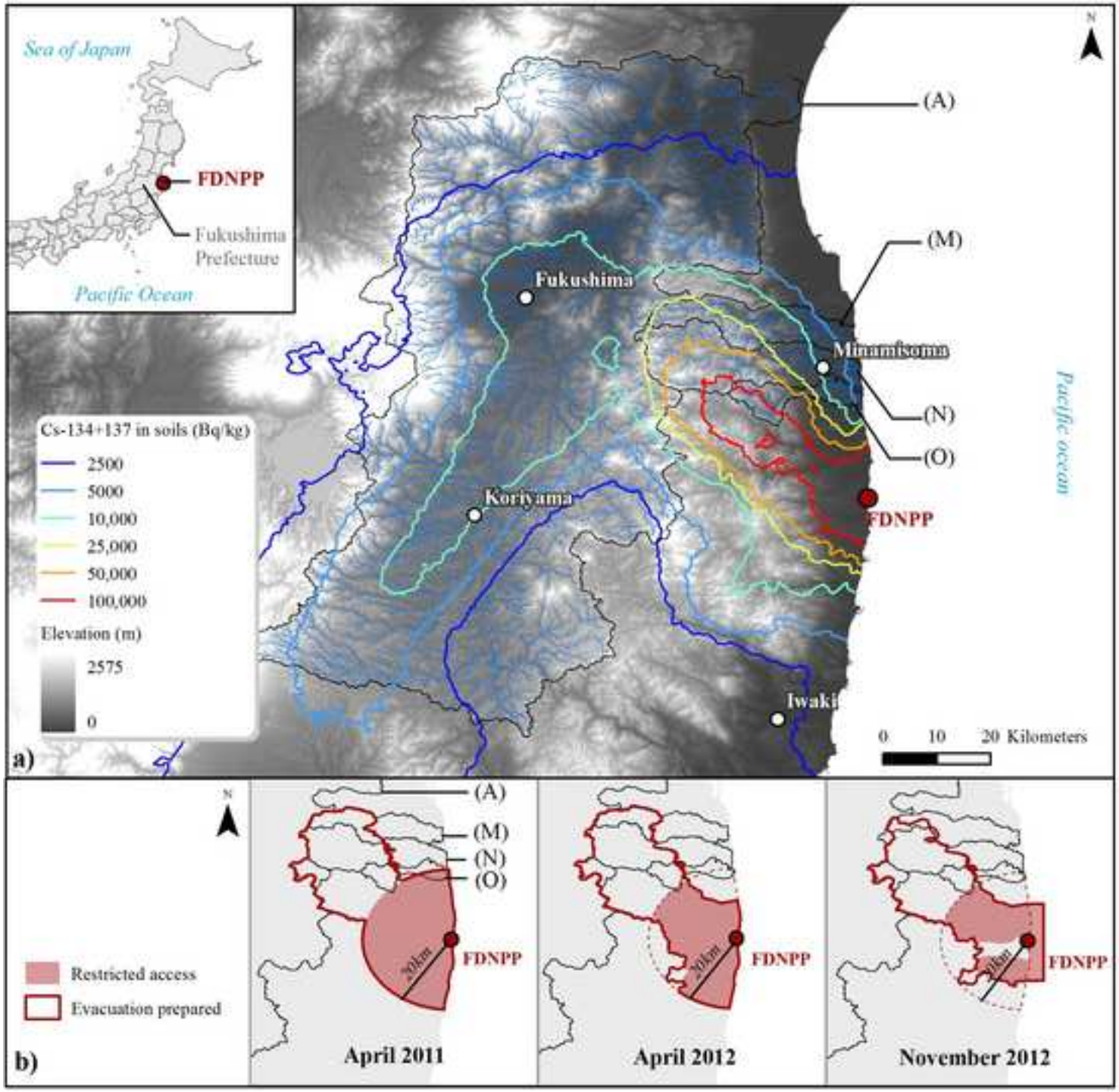

Figure 2 revised

Click here to download high resolution image

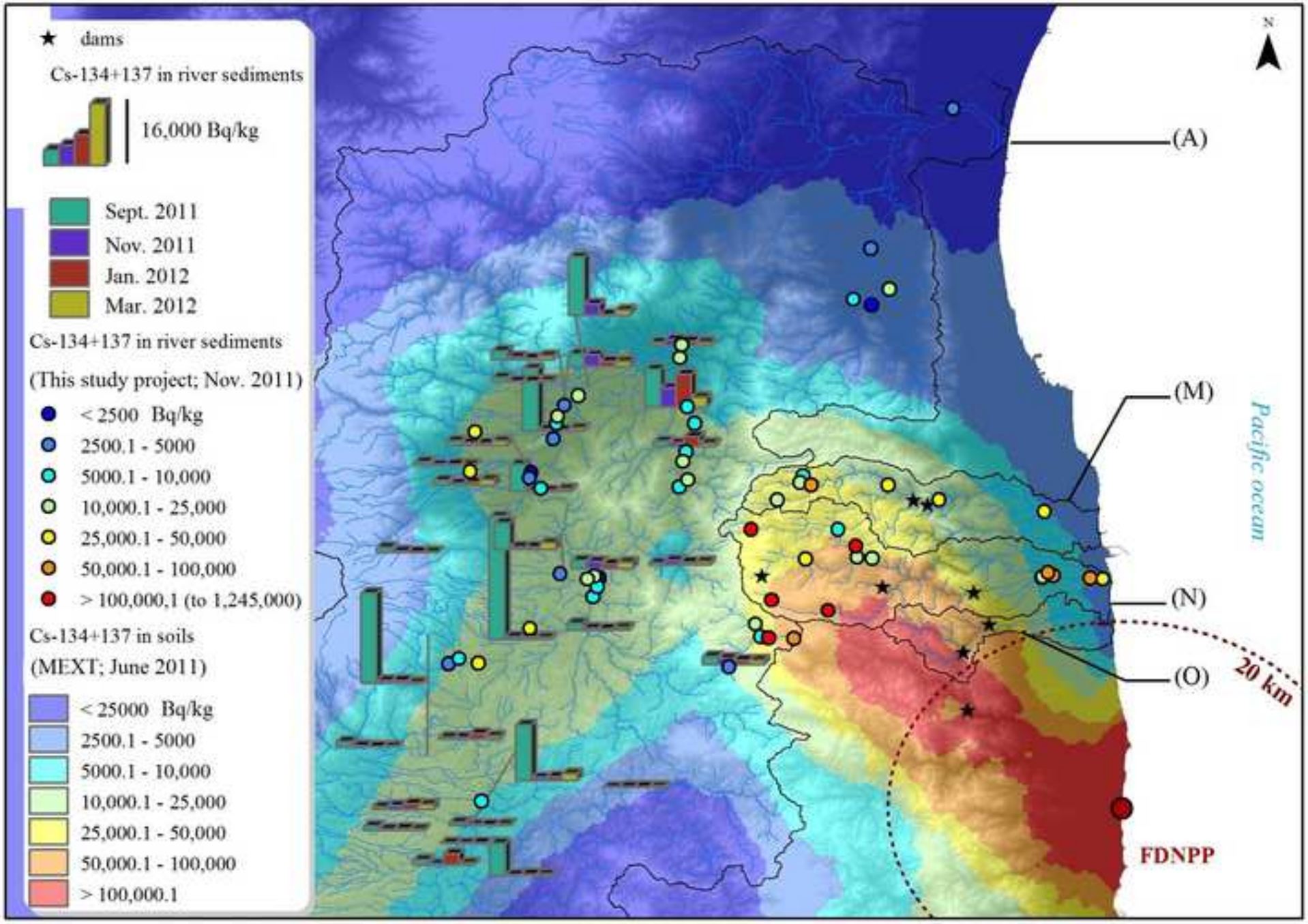

Figure 3

Click here to download high resolution image

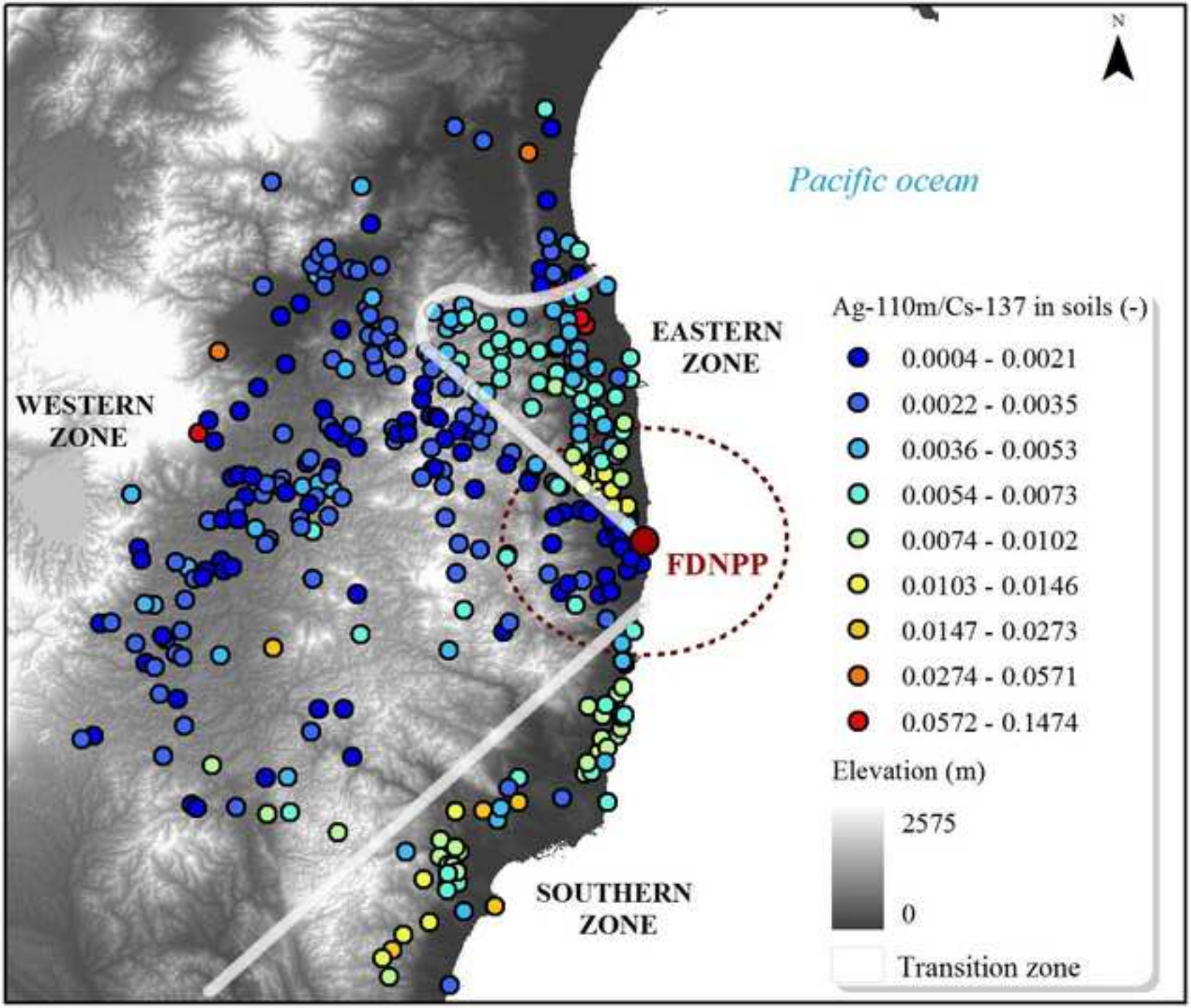

Figure 4

Click here to download high resolution image

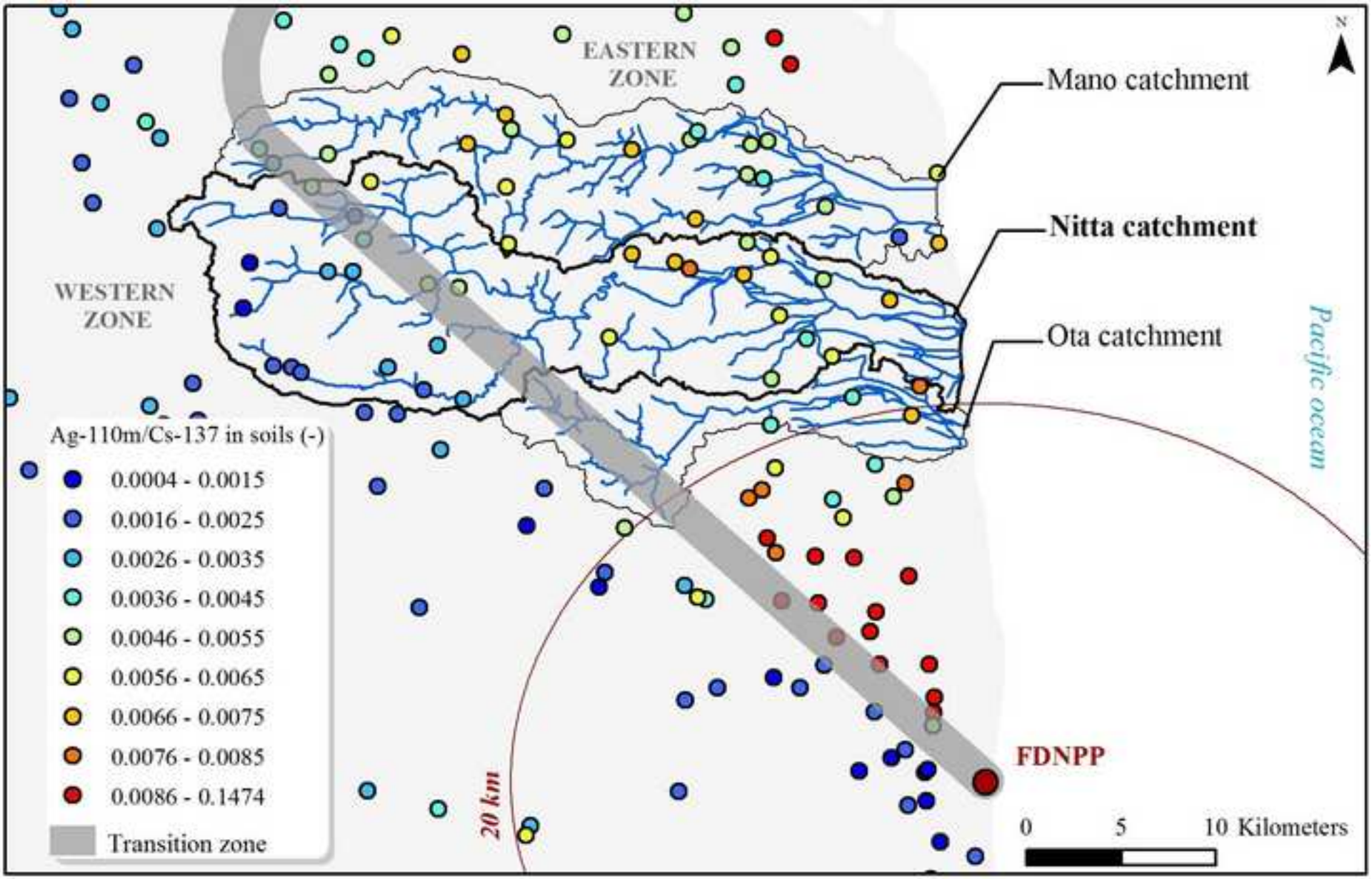

Figure 5

Click here to download high resolution image

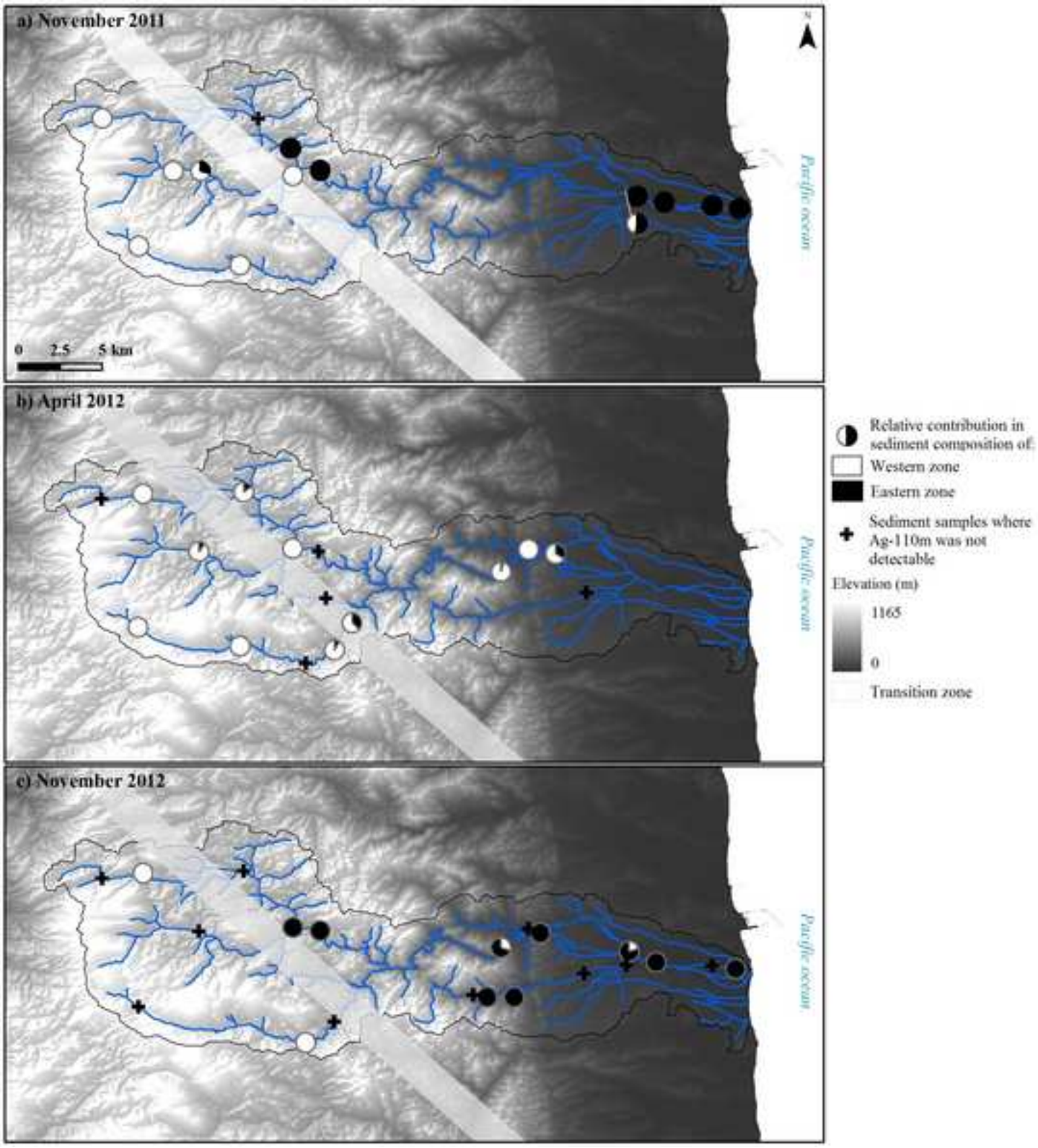

Figure 6

Click here to download high resolution image

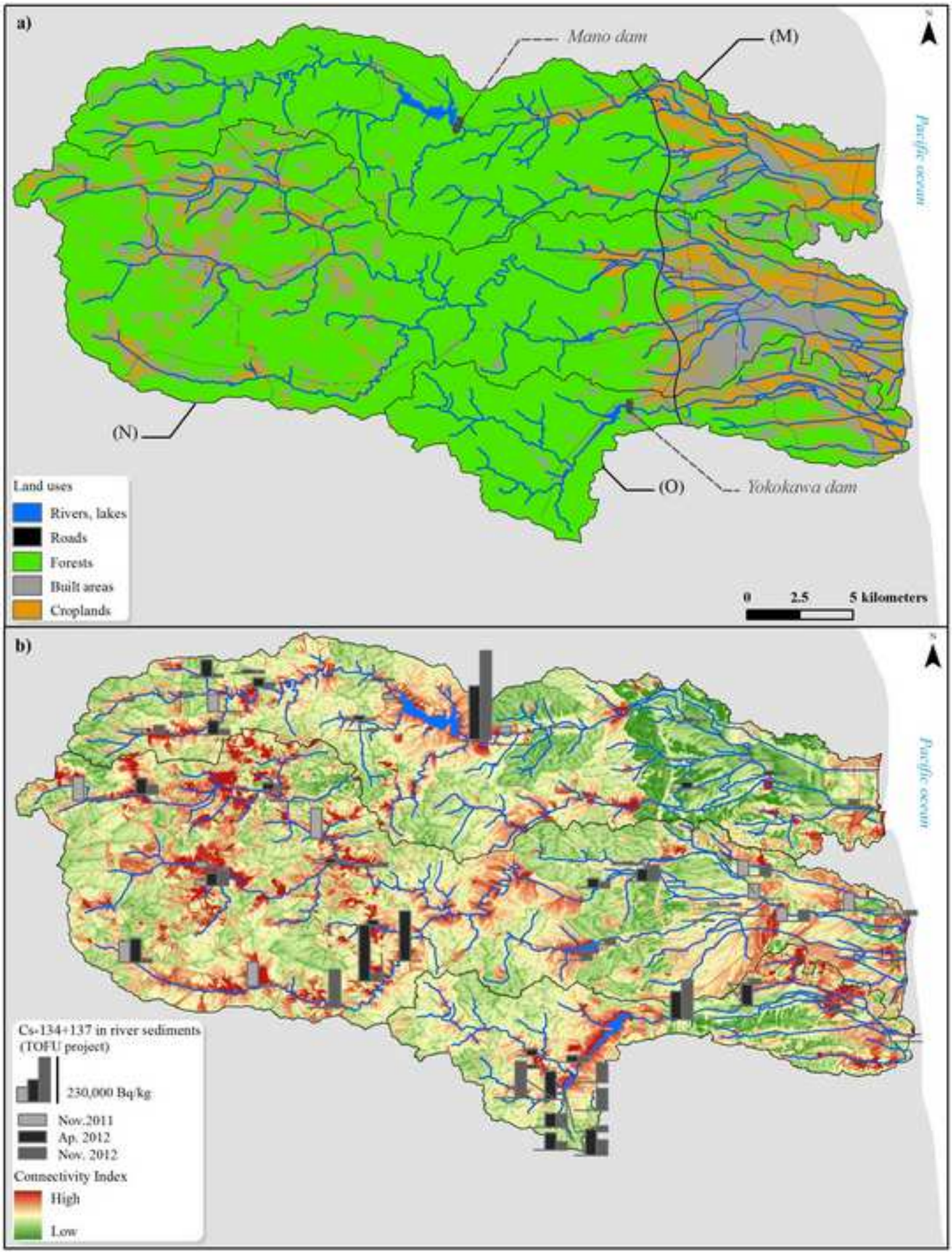

Figure 7 revised

Click here to download high resolution image

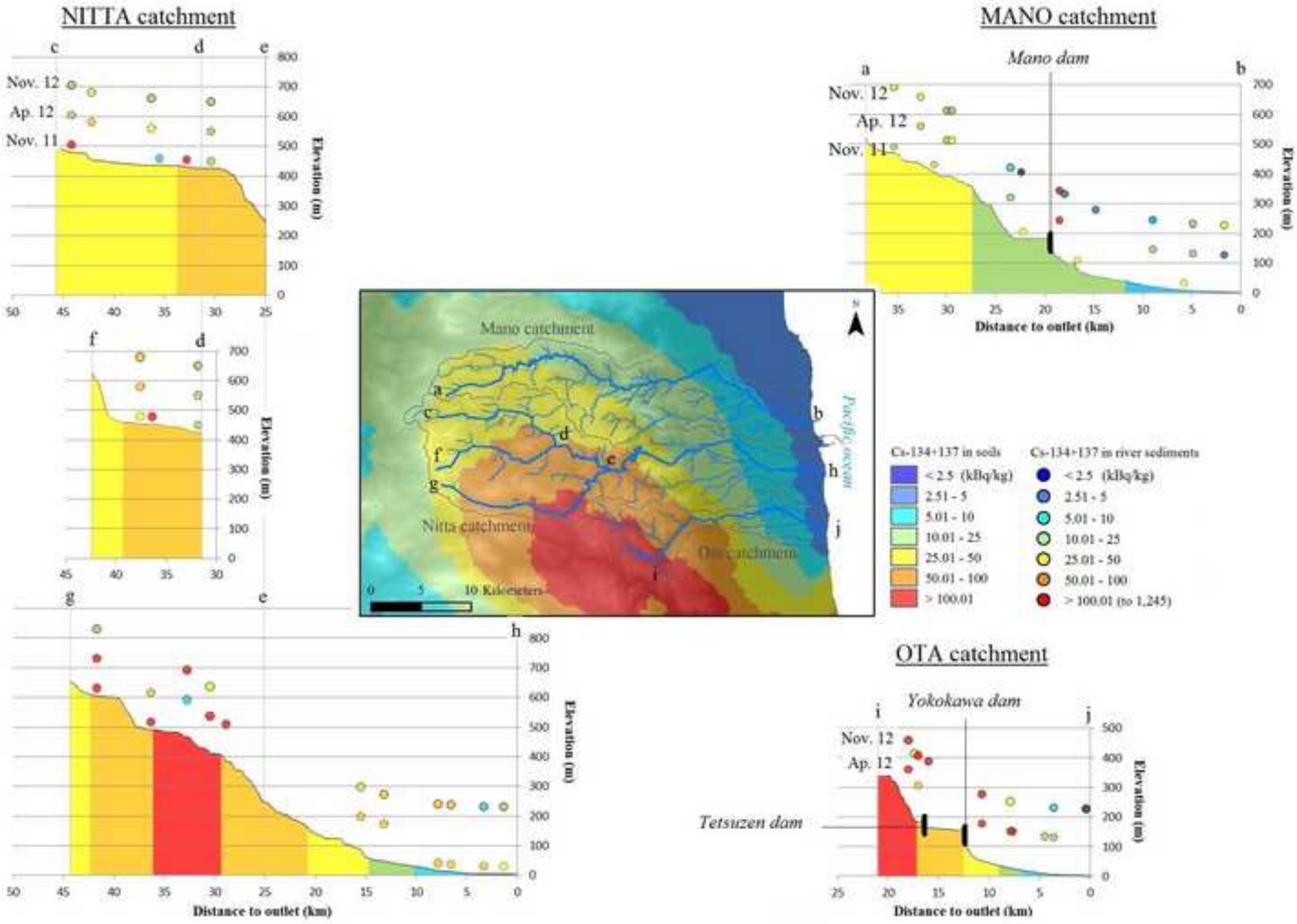

Figure 8

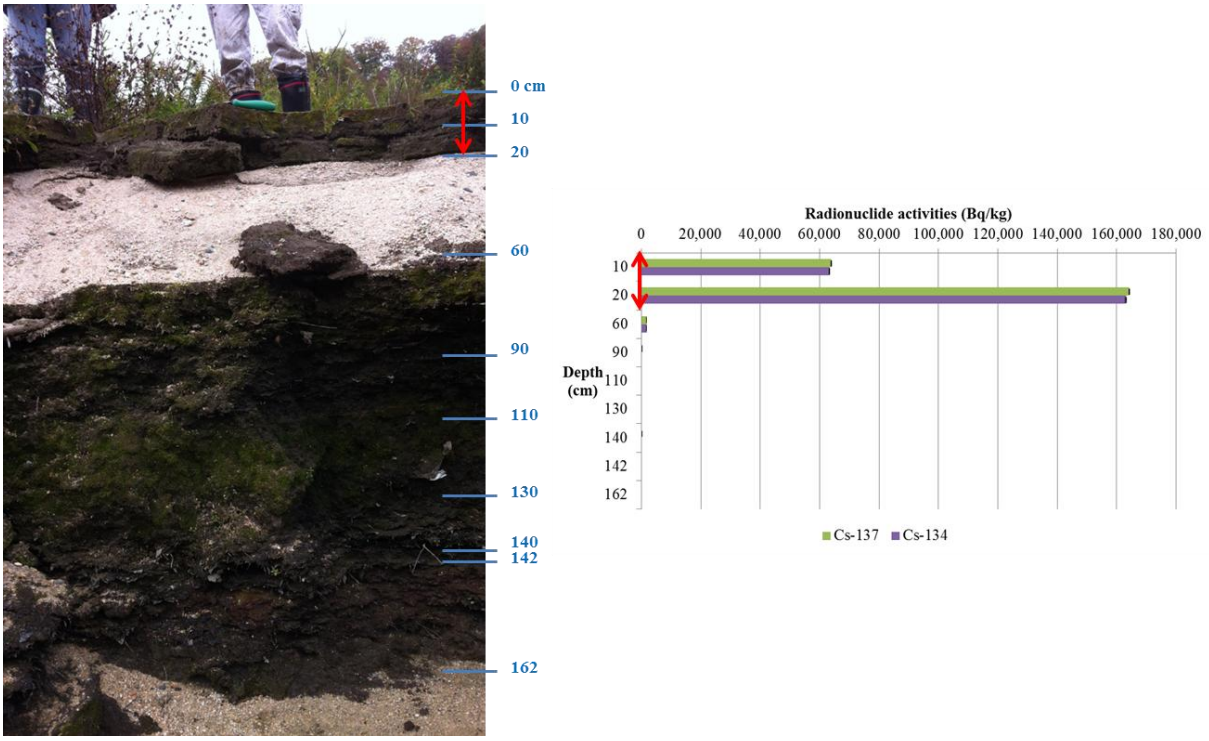
0 cm
10
20
60
90
110
130
140
142
162
Radionuclide activities (Bq/kg)
0
20,000
40,000
60,000
80,000
100,000
120,000
140,000
160,000
180,000
Depth (cm)
10
20
60
90
110
130
140
142
162
Cs-137
Cs-134

Table 1. Descriptive statistics of ^{110m}Ag:^{137}Cs ratio values measured in bulk soil under the authority of MEXT across Fukushima Prefecture (data located in a transition zone of 2-km width where there was a short-scale variability in ^{110m}Ag:^{137}Cs values between the 'western', the 'eastern' and the 'southern' zones were excluded).

Dataset	Western zone	Eastern zone	Southern zone
Count (-)	209	71	51
Minimum (-)	0.0004	0.0025	0.0024
Maximum (-)	0.1474	0.0969	0.0273
Mean (-)	0.0038	0.0090	0.0086
S.D. (-)	0.0112	0.0145	0.0044
Median (-)	0.0024	0.0058	0.0081

Table 2. Descriptive statistics of ^{110m}Ag:^{137}Cs ratio values measured in bulk soil under the authority of MEXT within the Nitta catchment (data located in the transition zone were excluded).

Dataset	Western zone *(Nitta catchment)*	Eastern zone *(Nitta catchment)*
Count (-)	12	14
Minimum (-)	0.0010	0.0041
Maximum (-)	0.0035	0.0082
Mean (-)	0.0023	0.0059
S.D. (-)	0.0008	0.0012
Median (-)	0.0024	0.0057

Graphical abstract

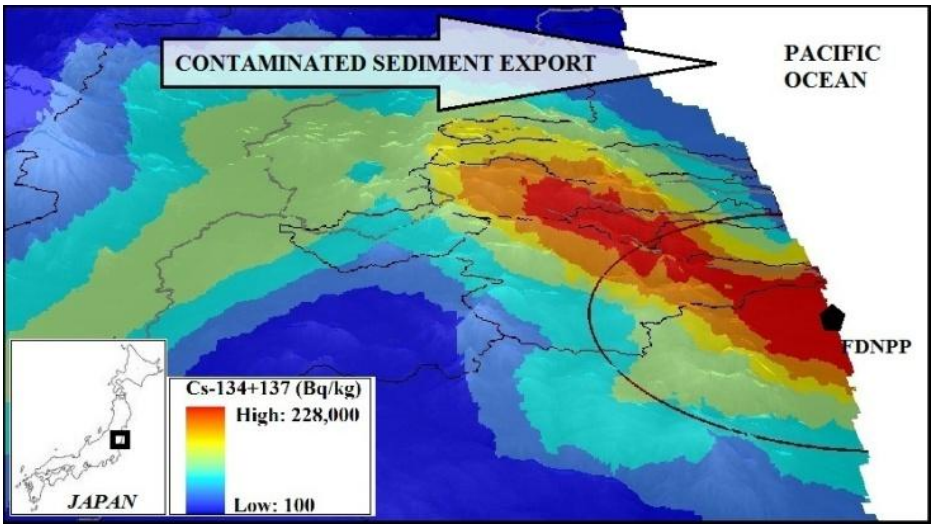

e-components Supplementary Fig. 1

Click here to download e-components: FigS1.doc